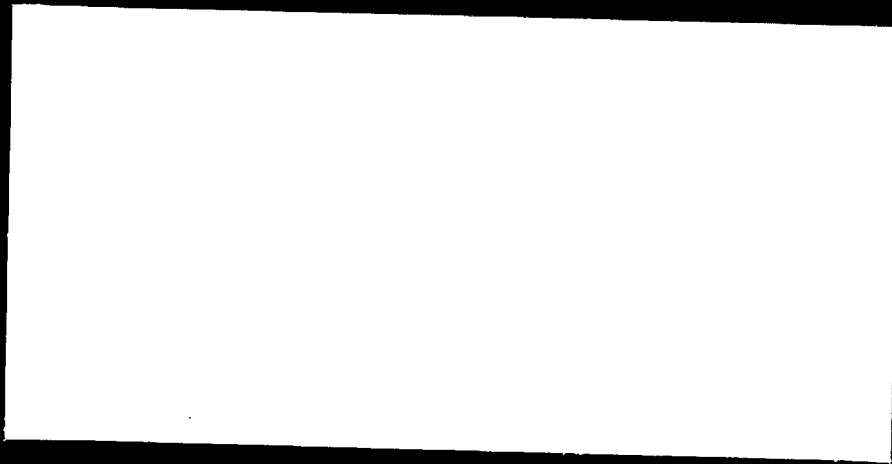


UNCLASSIFIED
DATE 01-10-2001

LOS ALAMOS SCIENTIFIC LABORATORY

OF THE UNIVERSITY OF CALIFORNIA
LOS ALAMOS, NEW MEXICO



CONTRACT W-7405-ENG. 36 WITH THE
U.S. ATOMIC ENERGY COMMISSION



THIS DOCUMENT CONTAINS UNCLASSIFIED INFORMATION

UNCLASSIFIED
DATE 01-10-2001

~~SECRET~~
SECRET

UNCLASSIFIED

LOS ALAMOS SCIENTIFIC LABORATORY
of the
UNIVERSITY OF CALIFORNIA

VERIFIED UNCLASSIFIED
Per LMR 6-20-79
By M. Ballega 9-12-96

Report written:
August 1955

PUBLICLY RELEASABLE
Per M. M. Jones FSS-16 Date: 7-2-96
By M. Ballega CIC-14 Date: 9-12-96

LA-1939

This document consists of 34 pages
of text and 12 figures. Series A.

c.3

INELASTIC CROSS SECTIONS AND $\bar{\nu}$
FOR SOME FISSIONABLE ISOTOPES

UNCLASSIFIED

Rwaney

Classification changed to UNCLASSIFIED
by authority of the U. S. Atomic Energy Commission
Per F. L. Cucchiara Dir. of Class.
Executive Order 10865 - Part 101 - (b)(7)

Report written by: 10-7-74

Work done by:

- H. A. Bethe
- J. R. Beyster
- R. E. Carter
- R. L. Henkel
- R. A. Nobles

- H. A. Bethe
- J. R. Beyster
- R. E. Carter

REPORT LIBRARY Ureala Salazar
11-5-74

AEC RESEARCH AND DEVELOPMENT REPORT

PHYSICS AND MATHEMATICS
(M-3679, 16th edition)

JAN 09 1987
JAN 10 1987

LOS ALAMOS NATL. LAB. LIBS.
3 9338 00348 0679

Energy Act of 1954. Its trans-

~~SECRET~~
SECRET

UNCLASSIFIED

UNCLASSIFIED

[REDACTED]

CONFIDENTIAL

PHYSICS AND MATHEMATICS
(M-3679, 16th edition)

Report distributed: NOV 4 1955	LA-1939
Los Alamos Report Library	1-20
AF Plant Representative, Burbank	21
AF Plant Representative, Seattle	22
AF Plant Representative, Wood-Ridge	23
Alco Products, Inc.	24
ANP Project Office, Fort Worth	25
Argonne National Laboratory	26-31
Armed Forces Special Weapons Project	32
Army Chemical Center	33
Atomic Energy Commission, Washington	34-36
Battelle Memorial Institute	37
Bettis Plant (WAPD)	38-41
Brookhaven National Laboratory	42-44
Bureau of Ships	45
Carbide and Carbon Chemicals Company (C-31 Plant)	46
Carbide and Carbon Chemicals Company (K-25 Plant)	47-48
Carbide and Carbon Chemicals Company (ORNL)	49-54
Chicago Patent Group	55
Chief of Naval Research	56
Columbia University (Havens)	57
Department of the Navy- Op-362	58
Directorate of Research (WADC)	59
Dow Chemical Company (Rocky Flats)	60
duPont Company, Augusta	61-63
Engineer Research and Development Laboratories	64
General Electric Company (ANPD)	65-68
General Electric Company, Richland	69-76
Goodyear Atomic Corporation	77-78
Hanford Operations Office	79
Headquarters, Air Force Special Weapons Center	80
Iowa State College	81
Knolls Atomic Power Laboratory	82-85
Mound Laboratory	86
National Advisory Committee for Aeronautics, Cleveland	87
National Bureau of Standards	88
Naval Medical Research Institute	89
Naval Research Laboratory	90-91
New Brunswick Area Office	92
New York Operations Office	93
New York University	94
North American Aviation, Inc.	95-97
Nuclear Development Associates, Inc.	98
Nuclear Metals, Inc.	99
Patent Branch, Washington	100
Phillips Petroleum Company (NRTS)	101-104
Powerplant Laboratory	105
Pratt & Whitney Aircraft Division (Fox Project)	106
Princeton University	107
Sandia Corporation	108
Sylvania Electric Products, Inc.	109
USAF Project RAND	110
U. S. Naval Postgraduate School	111
U. S. Naval Radiological Defense Laboratory	112
UCLA Medical Research Laboratory	113
University of California Radiation Laboratory, Berkeley	114-115
University of California Radiation Laboratory, Livermore	116-118
University of Rochester	119
Vitro Engineering Division	120
Walter Kidde Nuclear Laboratories, Inc.	121
Yale University	122
Technical Information Service, Oak Ridge (unbound copy for reproduction)	123
Special distribution:	
Manager, SFO (Russell Ball)	124

CONFIDENTIAL

[REDACTED]

CONFIDENTIAL

UNCLASSIFIED

UNCLASSIFIED

UNCLASSIFIED

ABSTRACT

The transmissions of neutrons through spherical shells of normal uranium, or alloy, and Pu^{239} are reported. One group of measurements was made using a pure fission neutron source produced by thermal neutrons in U^{235} , and the following detectors: U^{235} , U^{238} , Np^{237} fissions, and an $\text{Al}^{27}(\text{n},\text{p})\text{Mg}^{27}$ activation detector. The other group of measurements was made using monoenergetic neutrons from a Van de Graaff and principally a neutron-sensitive scintillation counter with a variable threshold. A U^{235} spiral fission counter was used also with this latter source to obtain information about $\bar{\nu}$ (average number of neutrons per fission) for different energies of the fission-inducing neutrons.

From both groups of measurements, the inelastic scattering cross sections have been determined according to methods developed in Los Alamos Scientific Laboratory Report LA-1429 (January 1955).

The non-elastic cross sections for these uranium and plutonium isotopes are given for various neutron energies, and values of $\bar{\nu}$, averaged over the fission spectrum, are also given.


For purposes of clarification in this report, we have adopted $\bar{\bar{\nu}}$ to indicate the double average.

ACKNOWLEDGMENTS

In general, the same people who assisted in the completion of our unclassified work, LA-1429, were helpful in this investigation. C. W. Johnstone, B. J. McCloud, A. S. Rawcliffe, and L. P. Grant helped with the many electronic problems. B. G. Carlson, Max Goldstein, Mrs. B. J. Masters, and Mrs. J. E. Bendt performed a large fraction of the numerical analyses.


UNCLASSIFIED

UNCLASSIFIED


 CONFIDENTIAL

CONTENTS

	Page
ABSTRACT	3
ACKNOWLEDGMENTS	3
CHAPTER 1 INTRODUCTION	5
CHAPTER 2 U ²³⁸ RESULTS	6
2.1 Cross Section Measured with Fission Neutrons and "28" (U ²³⁸) Threshold Detector	6
2.2 Cross Section Measured with a "37" (Np ²³⁷) Detector	9
2.3 Inelastic Cross Section Measured with an Al ²⁷ (n,p)Mg ²⁷ Threshold Detector	10
2.4 Two-Group Analysis of "37" Detector Transmission	12
2.5 Cross Sections Measured at 4.0 and 4.5 Mev Neutron Energies	16
2.6 Curve of Non-elastic Cross Section vs Neutron Energy	18
CHAPTER 3 INELASTIC CROSS SECTIONS AND $\bar{\nu}$ FOR ORALLOY (94 PERCENT U ²³⁵ , 5 PERCENT U ²³⁸ , AND 1 PERCENT U ²³⁴)	20
3.1 Fission Neutron Spectrum Results	20
3.1.1 Experimental Considerations	20
3.1.2 Method of Analysis of Data	21
3.2 Non-elastic Cross Section and $\bar{\nu}$ for Oralloy at 4.0 and 4.5 Mev Neutron Energies	26
CHAPTER 4 INELASTIC CROSS SECTIONS AND $\bar{\nu}$ FOR Pu ²³⁹	28
4.1 Fission Neutron Spectrum Results	28
4.2 Non-elastic Cross Sections and $\bar{\nu}$ at 4.0 and 4.5 Mev Neutron Energies	30
CHAPTER 5 CONCLUSIONS	31
REFERENCES	34

CONFIDENTIAL


SECRET

SECRET

Chapter 1

INTRODUCTION

The work of this report is an investigation of inelastic cross sections for fissionable isotopes, using previously developed methods. Experiments were done with two types of neutron sources: The external U^{235} fission neutron source at the LASL Water Boiler reactor, and monoenergetic Van de Graaff neutron sources of 4 and 4.5 Mev. The general experimental problems encountered with the fission neutron source are discussed in Chapters 9 and 10 of Los Alamos Scientific Laboratory Report LA-1429,¹ and these considerations for the Van de Graaff sources are discussed in The Physical Review.² Only those experimental problems which arose because of the fissionable nature of the isotopes will be considered in this report. Furthermore, since all of the theoretical methods necessary for the evaluation of these experiments were discussed in LA-1429, we will not derive the expression for sphere transmission, but merely give the equations used in our analyses.


The type of inelastic cross section with which we will be concerned in discussing fission spectrum data is that for the processes leading to removal of neutrons from a specific, rather broad, energy group. For the fission spectrum data the inelastic collision, or non-elastic, cross section includes capture, fission, and the inelastic scattering processes to below the energy threshold of the detector. For the monoenergetic Van de Graaff work the non-elastic cross section includes capture, fission, and all inelastic scattering.

For normal uranium, sufficient information was available from the work of the present report and other sources so that a fairly good curve of the variation of non-elastic cross section with energy could be constructed (Fig. 2.2, page 19).

It was also possible to obtain an idea of how $\bar{\nu}$, average number of neutrons per fission, varies with neutron energy by measuring fissionable sphere multiplications with a flat-response neutron counter at several neutron energies. This method is discussed in Chapter 8, LA-1429.¹ Our experimental results on $\bar{\nu}$ for the neutron energies considered in the present report are compared with those of other groups working on this problem.

SECRET

SECRET


 5710

Chapter 2
U²³⁸ RESULTS

2.1 Cross Section Measured with Fission Neutrons and "28" (U²³⁸) Threshold Detector


The cross section measured with fission neutrons and a "28" threshold detector (U²³⁸ detector) includes, by definition, all inelastic processes that remove neutrons to energies below the effective threshold of the "28" counter, which is 1.4 Mev. Chapter 7 of LA-1429 discusses this point at greater length.


The only experimental problem encountered here, beyond those given in LA-1429, was that of fissions of the U²³⁵ in the tuballoy spheres by low energy neutrons. This was shown to be negligible by two methods. With calibrated "25"* and "28" detectors, the ratio of the thermal to the fast flux at the sphere position in the room was measured. It was then possible to calculate the contribution to the sphere transmission of the fission neutrons caused by thermal neutron fission of U²³⁵. This turned out to be less than 0.001. The second method was to use spheres depleted in U²³⁵ to 1 part in 5000. Transmissions of these spheres were analyzed and gave very nearly the same cross sections for inelastic scattering as did the undepleted spheres.

The evaluation of the sphere transmissions was carried out by the methods of Chapters 4 and 8 of LA-1429. The actual expression used to relate cross sections and transmission was

$$\begin{aligned}
 T^{28} = & e^{-\sigma_3^t X} + \left(1 - e^{-\sigma_3^t X} \right) \left(\frac{\sigma_3^{el} + \sigma_3^f \nu_3 f_3}{\sigma_3^t} \right) \\
 & \times \left[\frac{\pi_1^3 + \frac{(1 - \pi_1^3) (\sigma_3^{et} + \sigma_3^f \nu_3 f_3) P_m^3}{(\sigma_3^{et} + \sigma_3^f \nu_3 f_3) P_m^3 + \sigma_3^{in} + \sigma_3^c + \sigma_3^f (1 - \nu_3 f_3)}}{\pi_1^3} \right]
 \end{aligned}
 \tag{2.1}$$

* The "25" detector contained 94 percent U²³⁵, 5 percent U²³⁸, and 1 percent U²³⁴. Its relative efficiency as a function of neutron energy was computed from the known fission cross sections of these isotopes.

67



 3110

where $\sigma_3^t, \sigma_3^{el}, \sigma_3^f, \sigma_3^{et}, \sigma_3^c, \sigma_3^{in}, \sigma_3^{tr}$ = total, elastic, fission, elastic transport, capture, inelastic scattering, and transport cross sections for group 3 neutrons

X = sphere thickness

f_3 = fraction of the fission neutron spectrum in energy group 3

π_1^3 = neutron escape probability after the first collision for group 3 neutrons, not including the effect of finite source to detector distance

$\hat{\pi}_1^3$ = neutron escape probability after the first collision, including the effect of finite source to detector distance

P_m^3 = neutron escape probability after the normal mode collision for group 3 neutrons, not including the effect of finite source to detector distance

\hat{P}_m^3 = neutron escape probability after normal mode collision, including the effect of finite source to detector distance

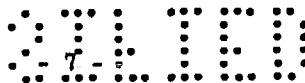
The subscript 3 on the cross sections is used to denote the energy group above the "28" detector threshold. The π_1^3 and $\hat{\pi}_1^3$ terms are computed using the actual differential cross section for elastic scattering explicitly. In P_m^3 one includes the effect of the asymmetric elastic scattering distribution by using a transport cross section instead of a total cross section.

Nomenclature becomes confusing at this point on the escape probabilities. The superscripts associated with escape probabilities in this report refer only to energy groups. No escape probabilities occur in any formulas squared or cubed.

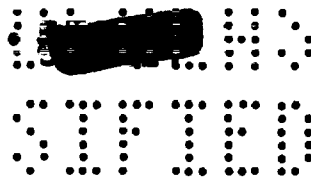
To compute the effect of fission neutrons on the sphere transmission, all the fissions were ascribed to group 3 neutrons. Thus, σ_3^f in Eq. 2.1 is equal to the fission cross section of U^{238} for a fission neutron spectrum divided by f_3 , the fraction of neutrons above the "28" detector threshold.

Auxiliary information used in the calculations was the average total cross section for group 3 neutrons, σ_3^t ; their elastic scattering angular distribution (relative only, not absolute values); the fission cross section of U^{238} for a fission spectrum; and ν_3 , the average number of neutrons emitted per fission caused by a neutron in energy group 3. The first two quantities were measured by Jurney and Zabel using a beam of fast neutrons from the Los Alamos fast reactor.³ The fission cross section of U^{238} for neutrons produced by the thermal fission of U^{235} was measured by Leachman and Schmitt,⁴ and $\nu_3 = 2.46$, the thermal $\bar{\nu}$ for U^{235} , was used.

Of the quantities in the analysis to which our result is sensitive, ν_3 is probably the least well known. For this reason we have given the final cross section in terms of a small correction term to allow for modification of the inelastic cross section in the event that ν_3 becomes better known. Present ideas⁵ indicate that ν_3 may be several percent above 2.46. Thus σ_3^{in}







may be as much as 4 percent greater than the number we are reporting. We have made no effort to use a ν_3 compatible with current ideas on the variation of $\bar{\nu}$ with energy because ν_3 actually enters here only in a rather small correction to the inelastic cross section. In the next chapter, however, we assume that $\bar{\nu}$ for U^{238} as well as U^{235} varies with neutron energy and we try to determine this variation.

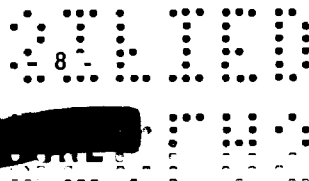
The results of the ten sphere transmission runs under somewhat differing experimental conditions are given in Table 2.1. The average of these values gives for the inelastic scattering (from group 3), plus capture cross section for group 3 neutrons

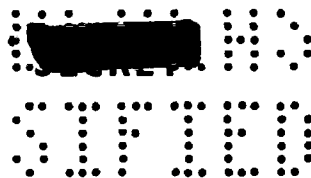
$$\sigma_3^{\text{in}} + \sigma_3^{\text{c}} = 2.09 + 0.305(\nu_3 - 2.46) \text{ barns}$$

TABLE 2.1
RESULTS OF TEN SPHERE TRANSMISSION RUNS

Outside diameter of sphere, inches	Sphere thickness, inches	Source distance, inches	T_{obs}^*	$\sigma_3^{\text{in}} + \sigma_3^{\text{c}}$, barns
8	3/8	10	0.9088	2.075
8	3/4	10	0.8160	2.068
8	3/4	20	0.8084	2.093
8	1-1/2	10	0.6449	2.045
8	1-1/2	20	0.6356	2.062
5	3/8	10	0.9087	2.069
5	3/4	10	0.8174	2.083
4	3/4	10	0.8027	2.108
4	3/8	10	0.9030	2.071
3-5/8	3/8	10	0.9067	2.132

* All transmissions were measured to an accuracy of ± 0.002 .





For the non-elastic cross section (fission added) we obtain

$$\sigma_3^{ne} = 2.64 + 0.305(\nu_3 - 2.46) \text{ barns}$$

The uncertainty in these values, exclusive of that due to the ν_3 uncertainty, is about 5 percent.

The data in Fig. 2.2 (page 19) are the non-elastic collision cross section at various energies (see section 2.6). Numerical integration of this curve over the fission spectrum and the U^{238} fission cross section gives an average non-elastic cross section of 3.00 barns. This is the cross section that one would expect to observe if all neutrons after an inelastic scattering had energies below the U^{238} fission threshold. Our measured value of 2.64 barns means that about 80 to 90 percent of the neutrons inelastically scattered by U^{238} are left with an energy below 1.4 Mev.

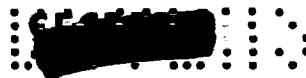
2.2 Cross Section Measured with a "37" (Np^{237}) Detector

The effective energy threshold of the "37" (Np^{237}) detector is about 0.7 Mev, and again the inelastic scattering cross section we measure is that for removal of neutrons to energies below this threshold. Here, however, we are undoubtedly counting a large number of neutrons which have made inelastic scatterings. This is indicated by the fact that the inelastic scattering cross section is about 1/2 of that measured with the "28" counter, yet 70 percent of the original fission neutrons detected in the "37" counter are also above the effective threshold of the "28" counter. Even though the spectrum above the "37" threshold is changing, we did not measure significantly different cross sections for different thicknesses of the tuballoy shell. This is entirely reasonable and has been observed before for many other non-fissionable elements. It is discussed in greater detail in Section 8.5 of LA-1429. For this investigation five shells of tuballoy varying in outside diameter from 8 to 4 inches and in thickness from 3/8 to 1-1/2 inches, were run. The over-all spread in the measured cross sections was 5 percent.

Fission of the U^{238} was included in the calculations, and, as in the previous section, ν_3 was taken as 2.46. Since the average $\bar{\nu}$ of U^{238} for the fission neutron spectrum may be about 10 percent different from this value, we include an appropriate correction term in our one-group cross section. The inelastic scattering plus capture cross section measured with the "37" detector is

$$\sigma^{in} + \sigma^c = 1.00 + 0.305(\nu_3 - 2.46) \text{ barns}$$




 3710

The non-elastic cross section is

$$\sigma^{ne} = 1.34 + 0.305(\nu_3 - 2.46) \text{ barns}$$

These cross sections are about 7 percent uncertain, exclusive of any uncertainty introduced by ν_3 .

This one-group method of interpreting the "37" counter transmission is of questionable value because it does not tell quantitatively and directly what energies the inelastically scattered neutrons have. A clearer understanding of this point may be obtained using a two-group method of evaluating the "37" detector transmissions. This is done in Section 2.4.

2.3 Inelastic Cross Section Measured with an Al²⁷(n,p)Mg²⁷ Threshold Detector


The experimental methods used for the non-fissionable elements with the Al²⁷(n,p)Mg²⁷ activation threshold detector were used for the measurements with the U²³⁸ spheres. This technique is discussed in Chapter 9 of LA-1429. The interpretation of the measured transmission was, however, slightly complicated by the fission processes in the shells.

The formulas used to evaluate the data are given next. The group of neutrons in the fission spectrum to which the aluminum activation detector is sensitive will be called group 4, and a subscript 4 will be given to all cross sections describing the behavior of these neutrons in the shell of tuballoy. Group 3 neutrons, as in Section 2.1, are defined here as those neutrons in the fission spectrum above the "28" detector threshold. Using the cross section definitions and analytical methods of Chapter 8, LA-1429, and Section 2.1 of this report, we can calculate the expected transmission of the uranium sphere, namely

$$T^{Al} = T + T_1 + T_2 + T_3$$

The first term is just the total number of group 4 neutrons escaping with neither a fission nor an inelastic scattering, and is

$$\begin{aligned}
 T = e^{-\sigma_4^{tr} X} + \left(1 - e^{-\sigma_4^{tr} X} \right) \frac{\sigma_4^{et}}{\sigma_4^{tr}} \left[P_1^4 + \left(1 - P_1^4 \right) \frac{\sigma_4^{et}}{\sigma_4^{tr}} P_2^4 \right. \\
 \left. + \frac{(1 - P_1^4)(1 - P_2^4)(\sigma_4^{et})^2 P_m^4}{\sigma_4^{tr} (\sigma_4^{in} + \sigma_4^c + \sigma_4^f + \sigma_4^{et} P_m^4)} \right] \quad (2.2)
 \end{aligned}$$

2110
 10.5


[REDACTED]

SECRET

The second terms, which correct for the counts due to fissions, consist of the following

$$\begin{aligned}
 T_1 &= \left(1 - e^{-\sigma_4^{tr} X} \right) \frac{\sigma_3^f \nu_3 f_3 P_1^3}{\sigma_4^{tr}} \\
 T_2 &= \frac{\left(1 - e^{-\sigma_4^{tr} X} \right) \sigma_3^f \nu_3 f_3 \left(1 - P_1^3 \right) \left(\sigma_3^{et} + \sigma_3^f \nu_3 f_3 \right) P_m^3}{\sigma_4^{tr} \left[\left(\sigma_3^{et} + \sigma_3^f \nu_3 f_3 \right) P_m^3 + \sigma_3^{in} + \sigma_3^c + \sigma_3^f - \sigma_3^f \nu_3 f_3 \right]} \\
 T_3 &= \frac{\left(1 - e^{-\sigma_4^{tr} X} \right) \sigma_4^{et} \left(1 - P_1^4 \right) \sigma_3^f \nu_3 f_3 \sigma_3^{tr} P_m^3}{\sigma_4^{tr} \left(\sigma_4^{in} + \sigma_4^c + \sigma_4^f + \sigma_4^{et} P_m^4 \right) \left[\left(\sigma_3^{et} + \sigma_3^f \nu_3 f_3 \right) P_m^3 + \sigma_3^{in} + \sigma_3^c + \sigma_3^f - \sigma_3^f \nu_3 f_3 \right]}
 \end{aligned}
 \tag{2.3}$$

The neutron source used in the experiment was external to the sphere, while the neutron detector was inside. Since we derived the transmission formulas with the source inside the sphere, it was necessary to utilize the three reciprocity conditions given in Section 8.1, LA-1429, namely:

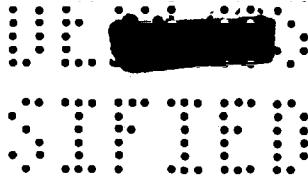
- (1) The probability of emission of group i neutrons when the source is outside the sphere must be the probability of detection of group i neutrons when we assume the detector outside.
- (2) The probability of detection of group i neutrons when the detector is inside the sphere must be the probability of emission of group i neutrons when the source is inside the sphere.
- (3) When source and detector are interchanged the transfer cross section from arbitrary energy groups j to i must be given the value of the original transfer cross section from i to j.

The term T_1 in Eq. 2.3 is the number of neutrons from a fission on the first collision in the shell that escape immediately and are counted in group 4. The term T_2 is the number of neutrons from a fission on the first collision that escape after one or more subsequent elastic collisions in the shell and are counted in group 4. The term T_3 is the total number of neutrons from fission on the second or subsequent collisions that eventually escape from the shell after any number of elastic scatterings and are detected in energy group 4.

Three shells of normal uranium were run with the aluminum threshold detector. Thickness varied from 3/8 to 1-1/2 inches, and the over-all spread in the cross section results was 6 percent. These experiments give for the inelastic scattering plus capture cross section

SECRET

[REDACTED]



of the neutrons above the effective threshold of the aluminum activation detector

$$\sigma_4^{\text{in}} + \sigma_4^{\text{c}} = 1.98 + 0.3(\nu_3 - 2.46) \text{ barns}$$

The non-elastic cross section (inelastic scattering plus capture plus fission) is then

$$\sigma_4^{\text{ne}} = \sigma_4^{\text{in}} + \sigma_4^{\text{f}} + \sigma_4^{\text{c}} = 2.80 + 0.3(\nu_3 - 2.46) \text{ barns}$$

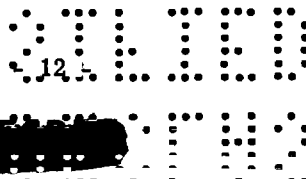
These numbers are about 7 percent uncertain if one neglects the uncertainty due to an inadequate knowledge of ν_3 .

The answers are undoubtedly very little affected by detection of neutrons after inelastic scattering, since most of the inelastic neutrons will have energies below the aluminum detector threshold. The average neutron energy for these measurements is around 6 Mev. It can be seen from Fig. 2.2 (page 19) that this cross section agrees quite well with our monoenergetic measurements on normal uranium at 7.0 Mev neutron energy.

2.4 Two-Group Analysis of "37" Detector Transmission

A two-energy group analysis similar to that of iron and cadmium in Sections 14.1 and 14.2 of LA-1429 is used here. The energy groups are 0.4 Mev to 1.4 Mev, called group 2, and above 1.4 Mev, called group 3. The group 3 constants are for the most part determined by the analysis of Section 2.1 of the present report. The value of $\sigma_3^{\text{in}} + \sigma_3^{\text{c}}$, for example, is 2.09 barns. Since σ_3^{c} is small and known, we can find the inelastic transfer cross section from group 3 to the two lower energy groups. We will call these transfer cross sections σ_{32}^{in} and σ_{31}^{in} , where the 32 subscript, for example denotes scattering from group 3 to group 2. The analysis of Section 2.1 does not tell us σ_{32}^{in} or σ_{31}^{in} , but only their sum.

The transmission formula for the "37" detector has two unknowns in it, σ_{31}^{in} or σ_{32}^{in} and $(\sigma_2^{\text{in}} + \sigma_2^{\text{c}})$, because the detector responds to neutrons in both energy groups. If we use transmissions for different shell thicknesses, we will weight the contribution to the shell transmission by each neutron group differently, and in principle obtain simultaneous equations for the two unknowns. The transmission with a "37" detector in two-group notation is



SECRET

$$\begin{aligned}
 T^{37} = F_3 T^{28} + F_2 \left[e^{-\sigma_2^{tr} X} + \left(1 - e^{-\sigma_2^{tr} X} \right) \frac{\sigma_2^{et}}{\sigma_2^{tr}} \left(P_1^2 + \frac{(1 - P_1^2) \sigma_2^{et} P_m^2}{(\sigma_2^{in} + \sigma_2^c + \sigma_2^{et} P_m^2)} \right) \right] \\
 + \frac{F_{32} \left(1 - e^{-\sigma_2^{tr} X} \right) \left(\sigma_{32} + \sigma_3 f \nu_3 f_2 \right) \sigma_3^{tr} P_m^3}{\left(\sigma_2^{et} P_m^2 + \sigma_2^{in} + \sigma_2^c \right) \left[\left(\sigma_3^{et} + \sigma_3^f \nu_3 f_3 \right) P_m^3 + \sigma_3^{in} + \sigma_3^c + \sigma_3^f \left(1 - \nu_3 f_3 \right) \right]}
 \end{aligned}
 \tag{2.4}$$

where T^{28} is given by Eq. 2.1
and

$$\begin{aligned}
 F_2 &= \frac{\sigma_2^{37} f_2}{\sigma_2^{37} f_2 + \sigma_3^{37} f_3} \\
 F_3 &= \frac{\sigma_3^{37} f_3}{\sigma_2^{37} f_2 + \sigma_3^{37} f_3} \\
 F_{32} &= \frac{\sigma_2^{37} f_3}{\sigma_3^{37} f_3 + \sigma_2^{37} f_2}
 \end{aligned}
 \tag{2.5}$$

The last term in Eq. 2.4 is the number of escaping group 2 neutrons produced by group 3 neutrons which either inelastically scatter or cause fission. Since the experiment is done with an external neutron source and internal neutron detector, we have to utilize in our analysis the three reciprocity conditions given in Section 2.3 to derive this term.

All quantities in Eq. 2.4 are either known from other sources of information or are known in terms of σ_{32}^{in} and $\sigma_2^{in} + \sigma_2^c$. Therefore, for each shell we select values of $\sigma_2^{in} + \sigma_2^c$ and solve for σ_{32}^{in} . A curve can then be plotted for each shell and the region of overlap of the curves obtained determines both σ_{32}^{in} and $\sigma_2^{in} + \sigma_2^c$. Figure 2.1 shows the results for the three tuballoy shells. It will be seen that we do not obtain a single curve for each shell, but rather a region of permissible values. This is caused by the statistical counting uncertainty in the measured shell transmissions. The best set of two-group constants for U^{238} is given in Table 2.2.

SECRET

SECRET
3170

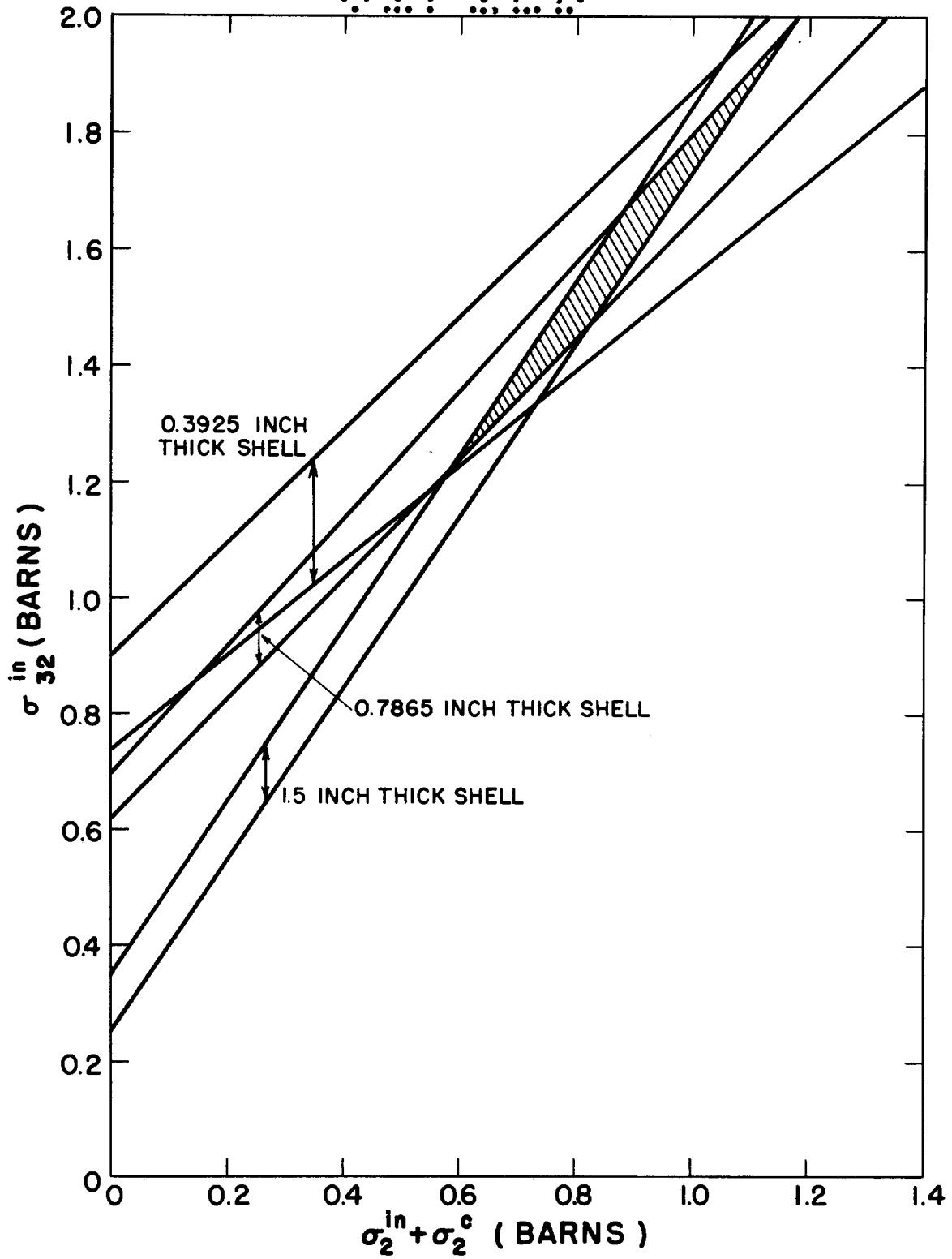


Fig. 2.1 σ_{32}^{in} vs $\sigma_2^{in} + \sigma_2^c$ with three tuballoy shells of different thicknesses.

SECRET
3170

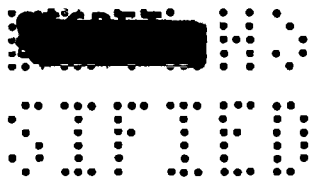


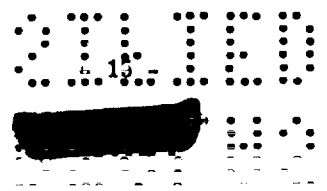
TABLE 2.2

TWO-GROUP CONSTANTS FOR U²³⁸*

Group 3 Values		Group 2 Values	
σ_3^t	7.60	σ_2^t	7.50
σ_3^{ne**}	2.64	σ_2^{ne**}	0.86 ± 0.30
σ_3^f	0.55	σ_2^f	0.0
σ_3^{el}	4.96	σ_2^{el}	6.64
σ_3^{et}	1.99	σ_2^{et}	4.32
σ_3^{tr}	4.63	σ_2^{tr}	5.18
σ_{32}^{in}	1.59 ± 0.35	σ_{21}^{in}	0.74
σ_{31}^{in}	0.46 ± 0.35	σ_2^c	0.12
σ_3^c	0.04		
ν_3	2.46		

* The underlined quantities are the ones primarily determined by the present measurements and computations.

** σ_i^{ne} is the group i non-elastic cross section composed of the sum of the group capture cross section, fission cross section, and inelastic scattering cross section for removal of neutrons from the group.




 13


The auxiliary data given were obtained from the following sources: The group 3 constants were obtained from Section 2.1 of this report. The total cross section in group 2, σ_2^t , was obtained by averaging the total cross section for uranium⁶ over the fission spectrum in group 2. The σ_2^c value, as well as σ_3^c , comes from averaging the fission spectrum in the two groups over the capture cross section for normal uranium.⁷ The ratio $\sigma_2^{et}/\sigma_2^{el}$ is that for the differential cross section for elastic scattering measured at 1.0 Mev by Walt and Barschall.⁸

The uncertainties in the quantities determined by this analysis are noted. The σ_{32}^{in} , σ_{31}^{in} , and $\sigma_2^{in} + \sigma_2^c$ values are not particularly well determined even after our analysis because we are not able to change the relative numbers of neutrons in groups 2 and 3 by a large amount with the shells of tuballoy available. However, this method does allow us to specify the relationship between σ_{32}^{in} and $\sigma_2^{in} + \sigma_2^c$ more exactly. Since these cross sections must lie in the shaded region in Fig. 2.1, we know that



$$\sigma_{32}^{in} = 1.30(\sigma_2^{in} + \sigma_2^c) + 0.47 \pm 0.05 \quad (2.6)$$


The B. G. Carlson S_4 method⁹ has also been used to evaluate these sphere transmission experiments. The same two energy groups are used and the problem is set up for an external neutron source such as we used in the experiments. With the same input parameters, the S_4 method computes the same shell transmission.

2.5 Cross Sections Measured at 4.0 and 4.5 Mev Neutron Energies

The technique for performing sphere transmission experiments at the Van de Graaff accelerator with monoenergetic neutron sources has been discussed in previous papers.² Essentially no variation of experimental method was required to perform the experiments on tuballoy. Transmission data were taken at between eight and ten energy thresholds simultaneously. These thresholds were spaced at energies from 90 percent of the incident neutron energy to 50 percent.

An analytic correction was applied for the fissions made in the sphere by the high energy neutrons, by the following method: The flux of fission spectrum neutrons at the threshold detector in the middle of the sphere was computed by the group methods of Chapter 8, LA-1429. The counts in the detector due to these neutrons can be determined if the sensitivity of the detector for fission neutrons relative to that for 4.0 or 4.5 Mev neutrons is known. The detector sensitivity was measured up to about 7 Mev neutron energy for each threshold, using the monoenergetic neutron sources, so that the relative sensitivity to fission neutrons and 4.0 or 4.5 Mev neutrons could be computed. The fission correction changed the inelastic cross section by about 10 percent. The uncertainty in the correction is about 30 percent.


 13



 CONFIDENTIAL

Experimental results are given in Table 2.3.

TABLE 2.3
CROSS SECTIONS MEASURED AT 4.0 AND 4.5 MEV NEUTRON ENERGIES

Neutron energy, Mev	Sphere outside diameter, inches	Sphere thickness, inches	Non-elastic cross section, barns
4.0	8	3/4	3.17 ± 0.20
4.5	5	3/4	3.12 ± 0.20
4.5	8	3/4	3.18 ± 0.20


Corrections for multiple scattering in the uranium shell and other smaller geometrical corrections had to be made to the transmission data. These corrections were computed by the methods of LA-1429, particularly Section 4.1. The auxiliary data required, namely the total neutron cross section and the angular distribution for elastic scattering, were measured.¹⁰


The cross sections in Table 2.3 are based on the transmission measurements at energy thresholds varying from 60 to 75 percent of the incident neutron energy. Measurements at higher thresholds require relatively large corrections for fission neutron counts, and lower thresholds can possibly count both inelastic neutrons and gamma rays. The measured inelastic cross section over the above threshold range is independent of threshold.

The experimental uncertainty in the values of Table 2.3 is determined by the transmission measurement uncertainty, the fission correction uncertainty, and uncertainties in quantities required in the multiple scattering analysis.

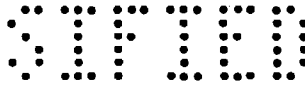
In addition to the transmission measurements with the high energy threshold detector, we measured the multiplication of a U²³⁸ shell with a "25" detector to determine $\bar{\nu}$ at 4.0 and 4.5 Mev, where $\bar{\nu}$ is the average number of neutrons emitted per fission of a U²³⁸ nucleus. This method is discussed in Chapter 8 of LA-1429. It is preferable to use a detector with a flat response for this type of measurement. However, if the sensitivity of the detector is known as a function of neutron energy, as it is for the "25" detector,* one may use a detector having a response that is not truly flat and include a correction in the calculations. We obtain $\bar{\nu} = 3.10 \pm 0.40$ at 4.5 Mev neutron energy. This is not in disagreement with the calculations of Leachman,⁵ which predict $\bar{\nu} = 3.05$. The uncertainty in $\bar{\nu}$ is mainly due to the low

*See footnote on page 6.

CONFIDENTIAL

 CONFIDENTIAL



 SECRET...



multiplication of the U^{238} sphere used in the experiments.

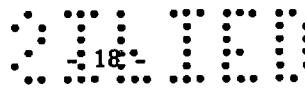
2.6 Curve of Non-elastic Cross Section vs Neutron Energy

The non-elastic cross section for U^{238} is shown in Fig. 2.2. The curve is drawn on the basis of presently available experimental data.^{8, 10-15} Each point is labeled with the reference number in this report of the original work from which the value was taken. The curve is a compromise in places where measurements by two different groups do not agree. The general shape of the curve of the non-elastic cross section of U^{238} is very similar to that obtained for tungsten or gold.


The behavior of the non-elastic cross section for U^{238} at energies below 1 Mev is quite uncertain at present and little effort was made to fit the points in this energy region. From 1 Mev to 7 Mev the cross section measurements by different methods are in fair agreement. The cross sections deduced by P. Olum¹¹ from disk scattering measurements certainly agree, within experimental errors, with the more recent measurements.

From 7 Mev to 14 Mev very little is known experimentally about the non-elastic cross section of U^{238} . In drawing the curve, we have selected a non-elastic cross section which is at most equal to the elastic cross section, despite the fact that some experimental data contradict this assumption. A straight line connecting 14 Mev values with 7 Mev values would give non-elastic cross sections larger than elastic cross sections. This seems quite unlikely,¹⁶ although not impossible.

In deciding on the best curve through the experimental data, it is clear that the authors have weighted the Los Alamos measurements more than those from other laboratories. For example, the Rice Institute¹³ data would indicate a non-elastic cross section several tenths of a barn higher than our curve at energies above about 3 Mev. The worst discrepancy between our curve and the Rice measurements¹³ is at 12.7 Mev. Obviously, further experiments are necessary to settle the behavior of the cross section above 7 Mev.



 -18-



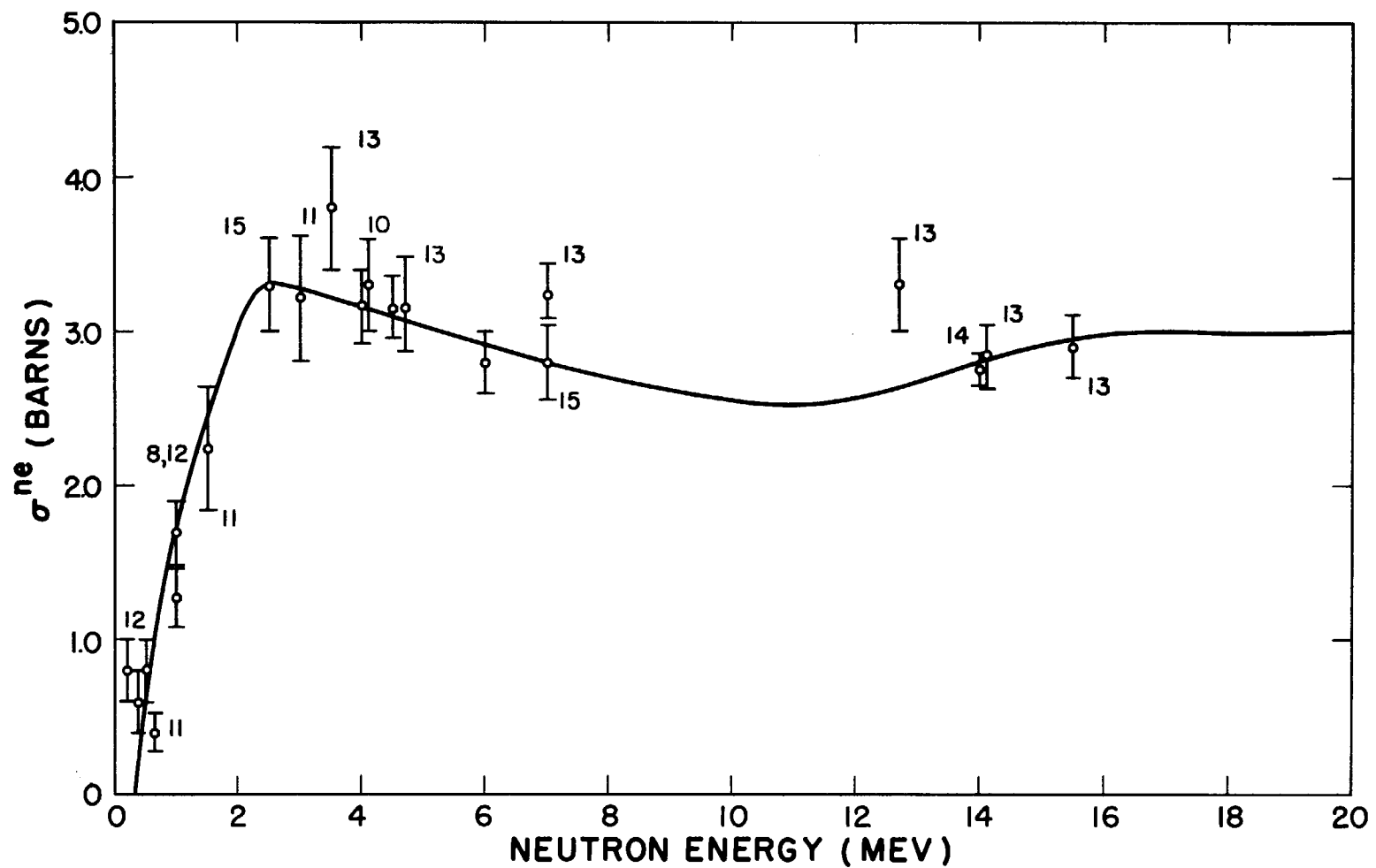



Fig. 2.2 Non-elastic cross section for U^{238} . Numbers appearing at the various points are the reference numbers in this report of the original works from which the values were taken. Values not marked by numbers are the result of the present work.


 3710

Chapter 3

INELASTIC CROSS SECTIONS AND $\bar{\nu}$ FOR ORALLOY (94 PERCENT U^{235} ,
 5 PERCENT U^{238} , AND 1 PERCENT U^{234})

3.1 Fission Neutron Spectrum Results

3.1.1 Experimental Considerations


The experimental procedure here is similar to that used for nonfissionable elements. Multiplications are measured by surrounding various neutron detectors with spheres of oralloy. The "28" and "37" threshold detectors and a "25" fission detector are used to measure the sphere multiplications. The external fission neutron source at the LASL Water Boiler was used.

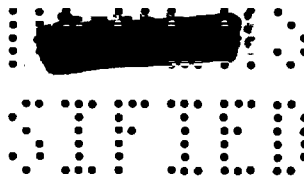
As might be expected, the experimental problems, particularly background problems, are somewhat more formidable with a "25" counter and with oralloy shells than with tuballoy shells. This background is of two types: (1) that emerging from the reactor and (2) that produced by room scattering of source neutrons. For simplicity in discussion, we can divide both of these backgrounds into 3 major energy groups: (a) thermal neutrons, (b) epi-thermal or resonance neutrons, and (c) fast neutrons with an energy distribution different from the fission spectrum.

The thermal neutrons could be excluded easily from both the oralloy shells and "25" counter with thin cadmium cups whose transmissions could be computed from the known cadmium inelastic cross sections.¹

Most of the fast neutrons were from room scattering (type 2). These could not be removed entirely, but could be minimized by measuring the sphere transmissions close to the source. In LA-1429, Sections 6.1 and 10.2, we had shown that we could accurately compute the obliquity correction at 5 inches and that the fast neutron background there was quite small, so this position was chosen for the measurements reported here.

This 5 inch position was also a compromise to make the epi-thermals of types 1 and 2 approximately equal, but they still caused the most serious problem, and so will be discussed in more detail. These neutrons can produce two effects: (1) with no shell (except cadmium) around the "25" counter they can cause counts directly and (2) with a cadmium-covered oralloy shell around any of our detectors, they can produce fissions in the shell, and the resulting

3710




neutrons may then be counted. This latter process converts epi-thermal neutrons into fission spectrum neutrons with a much lower efficiency for counting in a "25" detector, but an infinitely higher efficiency for counting in a "28" detector.

To study these various effects, we made an 8 inch diameter, thin aluminum, double-walled spherical can packed with a 1/8 inch thickness of B^{10} . This spherical shell of B^{10} attenuated the fission spectrum neutrons by only about 1 percent, but attenuated the epi-thermal neutrons by a factor of about 100. When the transmission of a cadmium-covered or alloy sphere was run inside of this B^{10} shell with a "28" counter, it was the same, within statistical errors, as a similar measurement not using the B^{10} shell. This indicates that the epi-thermal neutron fission effect in the or alloy shell is small for all detectors even with no B^{10} . However, when a similar set of measurements was made with a cadmium-covered "25" counter, the presence of the B^{10} shell made a large change in transmission. This effect in the "25" counter measurements was due primarily to the epi-thermal neutrons causing counts when both the B^{10} shell and or alloy shell were absent.

As an extra precautionary measure we made a small 1/4 inch thick sintered B^{10} sphere which was fitted permanently around the "25" detector. With this detector, the 8 inch diameter B^{10} shell had no measurable effect on the transmissions of or alloy spheres, but in order to make even smaller any fission effect, we ran all sphere transmissions inside of the 8 inch diameter B^{10} shell.

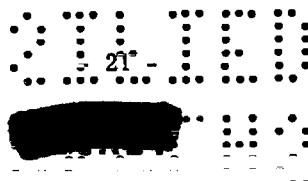
Most of the background emerging from the reactor was subtracted by measuring the sphere transmissions, inside of the B^{10} shell, with the U^{235} source plate replaced by a pseudo-source which had similar scattering characteristics. One must be a little careful in doing this with a "25" counter because the resonance energy neutrons in the beam are strongly absorbed by the U^{235} source plate, and therefore emerge to be counted only when the source plate is removed. The relatively large amount of B^{10} around the sphere and counter absorbed most of these neutrons, so that in the present experiments the error was quite small.


It should be emphasized that the measured transmissions of the or alloy spheres, particularly with the "25" counter, are subject to considerably more uncertainty than the statistical uncertainty of about 0.2 percent, because of the problems of eliminating or evaluating these backgrounds.

The estimated upper limit on the remaining error in transmission due to backgrounds is 0.005 when these two B^{10} spheres are used as described.

3.1.2 Method of Analysis of Data

Our approach here will be somewhat different from that in Chapter 2, where we considered the various threshold detectors separately. We will try to satisfy simultaneously the




 CONFIDENTIAL

sphere transmissions measured with the three detectors by adjusting the important cross sections in our three neutron groups: Group 1, 0 to 0.4 Mev; Group 2, 0.4 to 1.4 Mev; Group 3, 1.4 to ∞ . We must really consider all three transmissions together because fission couples the three groups together so that changes in one group will affect the number of neutrons escaping in another group.

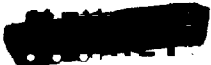
We will endeavor to obtain three quantities from our analysis. From the "25" detector analysis we obtain $\bar{\nu}$, the average number of neutrons produced per fission in or alloy by a fission spectrum neutron. Actually, as mentioned previously in this report and also in Chapter 8, LA-1429, $\sigma^f(\bar{\nu}-1) - \sigma^c$ * is the quantity determined by the or alloy sphere multiplication. However, since σ^f is known quite well and σ^c is small and fairly well known, we actually determine $\bar{\nu}$ from our analysis. The "28" detector transmission gives us the cross section for removal of neutrons from group 3 by inelastic scattering, namely, σ_3^{in} , since σ_3^c is quite small and known approximately. From the "37" detector transmission we determine $\sigma_2^{\text{in}} + \sigma_2^c$. Actually, we have one more unknown present in the analysis than we have independent equations. This additional unknown is $\sigma_{32}^{\text{in}}/\sigma_{31}^{\text{in}}$, the ratio of the cross section for transfer by inelastic scattering from group 3 to group 2, to the cross section for transfer from group 3 to group 1. For this we use a ratio which is consistent with that determined experimentally for U^{238} . If an error were made in our selection for this ratio, only $\sigma_2^{\text{in}} + \sigma_2^c$ will be affected to a first approximation, not $\bar{\nu}$ or σ_3^{in} . All other three-group constants required for the analysis are fairly well known quantities. Furthermore, the uncertainties in these quantities can introduce relatively little error into the determination of our unknowns.

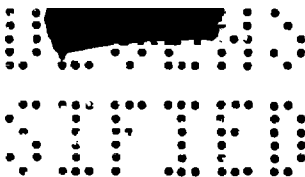
Of course the "25" detector is really not a flat response counter and for that reason is not ideal for these experiments. However, the average detector sensitivity in our three energy groups is computed for a fission spectrum shape and used to take into account the variation from flat response. This actually turns out to be a very small consideration. Transmissions computed for a flat response detector are less than 1 percent different from those including the "25" detector sensitivity explicitly.

The three-group formulas for our analysis are derived following the methods of Chapter 8, LA-1429. The analysis assumes an equivalent three energy group neutron source inside of the sphere because the experiment is done with an external neutron source. In the derivation of formulas, the three conditions in Section 8.1 of LA-1429, necessary for legitimate interchange of source and detector, will be satisfied.

Let us now consider formulas for a "25" detector. We designate P_1^{25} , P_2^{25} , and P_3^{25} as the detection sensitivities of our neutron detector in energy groups 1, 2 and 3. The terms

*The average refers to the average value of this quantity over the fission neutron spectrum.

22

 CONFIDENTIAL



f_1 , f_2 and f_3 are the emission probabilities of groups 1, 2 and 3 respectively, as well as being the fractions of the fission neutron spectrum in groups 1, 2 and 3. Equation 8.20 of LA-1429 gives the following three equations for the integrated neutron flux per energy group, ψ_i

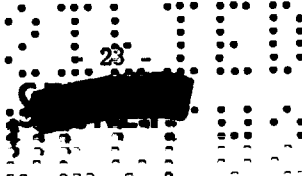
$$\begin{aligned} \psi_3 \left[\sigma_3^{\text{in}} + \sigma_3^{\text{c}} + \sigma_3^{\text{f}}(1 - \nu_3 f_3) + P^3 \sigma_{33} \right] &= P_3^{25} (1 - e^{-\sigma_3^{\text{tr}} X}) \\ &+ \psi_2 \sigma_{23} (1 - P^3) + \psi_1 \sigma_{13} (1 - P^3) \\ \psi_2 \left[\sigma_2^{\text{in}} + \sigma_2^{\text{c}} + \sigma_2^{\text{f}}(1 - \nu_2 f_2) + P^2 \sigma_{22} \right] &= P_2^{25} (1 - e^{-\sigma_2^{\text{tr}} X}) \\ &+ \psi_3 \sigma_{32} (1 - P^2) + \psi_1 \sigma_{12} (1 - P^2) \\ \psi_1 \left[\sigma_1^{\text{c}} + \sigma_1^{\text{f}}(1 - \nu_1 f_1) + P^1 \sigma_{11} \right] &= P_1^{25} (1 - e^{-\sigma_1^{\text{tr}} X}) \\ &+ \psi_3 \sigma_{31} (1 - P^1) + \psi_2 \sigma_{21} (1 - P^1) \end{aligned} \quad (3.1)$$

where

$$\begin{aligned} \sigma_{33} &= \sigma_3^{\text{et}} + \sigma_3^{\text{f}} \nu_3 f_3 \\ \sigma_{32} &= \sigma_2^{\text{f}} \nu_2 f_3 \\ \sigma_{31} &= \sigma_1^{\text{f}} \nu_1 f_3 \\ \sigma_{22} &= \sigma_2^{\text{et}} + \sigma_2^{\text{f}} \nu_2 f_2 \\ \sigma_{23} &= \sigma_3^{\text{f}} \nu_3 f_2 + \sigma_{32}^{\text{in}} \\ \sigma_{21} &= \sigma_1^{\text{f}} \nu_1 f_2 \\ \sigma_{11} &= \sigma_1^{\text{et}} + \sigma_1^{\text{f}} \nu_1 f_1 \\ \sigma_{12} &= \sigma_2^{\text{f}} \nu_2 f_1 + \sigma_{21}^{\text{in}} \\ \sigma_{13} &= \sigma_3^{\text{f}} \nu_3 f_1 + \sigma_{31}^{\text{in}} \end{aligned} \quad (3.2)$$

All cross sections used in these formulas are defined in Sections 2.1 and 2.3. Average escape probabilities are determined for each energy group. The superscripts on the escape probabilities refer to these energy groups and do not mean that squares or cubes of escape probabilities occur in the formulas.

For a given set of three-group cross sections we compute ψ_1 , ψ_2 , and ψ_3 from Eq. 3.1



[REDACTED]

and then use these to solve for the neutrons actually escaping from the shell in the three energy groups, namely

$$\begin{aligned}
 q_1 &= P_1^{25} e^{-\sigma_1^{tr} X} + (\psi_1 \sigma_{11} + \psi_2 \sigma_{21} + \psi_3 \sigma_{31}) P_1^{\wedge 1} \\
 q_2 &= P_2^{25} e^{-\sigma_2^{tr} X} + (\psi_1 \sigma_{12} + \psi_2 \sigma_{22} + \psi_3 \sigma_{32}) P_2^{\wedge 2} \\
 q_3 &= P_3^{25} e^{-\sigma_3^{tr} X} + (\psi_1 \sigma_{13} + \psi_2 \sigma_{23} + \psi_3 \sigma_{33}) P_3^{\wedge 3}
 \end{aligned}
 \tag{3.3}$$

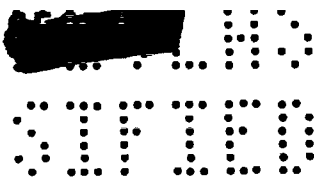
The sphere transmission for our "25" detector is

$$T^{25} = \frac{f_1 q_1 + f_2 q_2 + f_3 q_3}{f_1 P_1^{25} + f_2 P_2^{25} + f_3 P_3^{25}}
 \tag{3.4}$$

The formulas for the transmissions with the "28" and "37" detectors follow easily from this by merely replacing P_1^{25} , P_2^{25} , and P_3^{25} with the appropriate probabilities for these detectors. To speed up the computing problem, these equations have been coded for the CPC machines at Los Alamos. If one uses the B. G. Carlson S_4 method⁹ with three energy groups to compute these transmissions, one obtains essentially the same answers as we get by this method for, of course, the same input parameters.

Although it is not obvious from our equations, it is nevertheless true that the actual computed transmissions are not very sensitive to most of the auxiliary data which one uses. The sources of this auxiliary information used in our computing problem will next be noted. Total cross sections σ_1^t , σ_2^t , and σ_3^t were averages of the total cross sections from LA-1493¹⁷ over the portions of the fission neutron spectrum corresponding to our individual energy groups. The σ_1^f , σ_2^f , and σ_3^f were similar averages of the U^{235} and U^{238} fission cross sections using the latest fission cross section data in LA-1714.¹⁸ The $(\sigma^{et}/\sigma^{el})_3$ was obtained from an angular distribution of elastic scattering measured by Journey and Zabel³ for U^{238} , $(\sigma^{et}/\sigma^{el})_2$ is essentially the Walt and Barschall⁸ measurement at 1.0 Mev neutron energy for U^{238} , and $(\sigma^{et}/\sigma^{el})_1$ is estimated from the trend of the previous ratios with energy and also recent measurements by Los Alamos Group P-3.¹² The three-group capture cross sections are those estimated from bomb data by Hansen and Engle.¹⁹ These capture cross sections may not be the best set. Bomb data give a capture to fission average ratio of 0.15, while an

.



average of 0.11 is used here and the difference is attributed to the presence of a degraded fission spectrum in a bomb. Recent Argonne data²⁰ from the EBR (Experimental Breeder Reactor) indicate that the capture to fission ratio varies appreciably with spectrum, but indicate that 0.11 may be too high a ratio from an undegraded fission spectrum in U²³⁵. Clearly this ratio has a large uncertainty at present. The $\bar{\nu}$ selections for each energy group were made as follows: In groups 1 and 2, group averages based on Leachman's⁵ calculations were used and ν_3 only was adjusted on the basis of the oralloy sphere multiplication with the "25" detector. All escape probabilities were read from the general sets of curves in Chapters 5 and 6 of LA-1429.

The best set of three-group constants for 94 percent enriched oralloy is given in Table 3.1. With these cross sections, we calculate the same oralloy sphere multiplications as we measured experimentally with our three fission detectors. Multiplications for three shells were measured. The shells varied in size from 4 kilograms to 25 kilograms of material.

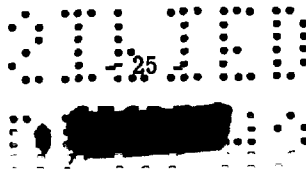
Using these same three-group constants in a Carlson S₄ critical radius calculation for an untamped oralloy sphere gives a critical radius of 8.644 cm. The experimentally measured critical radius of Godiva (untamped oralloy sphere) was 8.69 cm.


TABLE 3.1

AVERAGE THREE-GROUP CROSS SECTIONS FOR 94 PERCENT ENRICHED ORALLOY*

Group 3 values		Group 2 values		Group 1 values	
σ_3^{ne}	<u>2.59 ± 0.18</u>	σ_2^{ne}	<u>1.85 ± 0.22</u>	σ_1^c	0.33
σ_3^f	1.24	σ_2^f	1.15	σ_1^f	1.44
σ_3^{et}	2.01	σ_2^{et}	3.31	σ_1^{et}	6.66
σ_3^{tr}	4.60	σ_2^{tr}	5.16	σ_1^{tr}	8.45
σ_{32}^{in}	<u>0.85</u>	σ_{21}^{in}	<u>0.52</u>	ν_1	2.49
σ_{31}^{in}	<u>0.42</u>	σ_2^c	0.18		
σ_3^c	0.08	ν_2	2.54	$\bar{\nu}$	<u>2.60</u>
ν_3	<u>2.65</u>				

*The underlined quantities are the ones primarily determined by the present measurements and computations.




 3110

At this point it seems in order to make some comments on the use of these three-group constants for oralloy. Many of the auxiliary data are from preliminary or non-precise experiments or computations and may change in the course of time. As noted above, there is already considerable disagreement in the value of $\alpha = \sigma^c / \sigma^f$.

However, the numbers in Table 3.1 are consistent within themselves and, as mentioned, predict a critical mass with relatively high accuracy. Therefore, if new values for some of the auxiliary data become available at a later date, one is not necessarily justified in changing only those numbers and expecting to compute critical masses even more accurately. It might be necessary to adjust all of the remainder of the numbers in Table 3.1 in order that self-consistency be maintained. For example, there are now several sets of three-group constants,¹⁹ all slightly different, but each set predicting the correct critical mass for untamped oralloy.

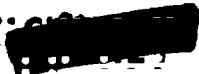
Our set of constants differs from previous sets of three-group constants in that we have used for our auxiliary data the most recent values for differential cross sections and have included a $\bar{\nu}$ which varies with neutron energy. In addition to satisfying critical mass measurements, our set of constants will also correctly predict multiplications for subcritical shells of oralloy measured with various neutron detectors. Not all of the previous sets of constants will do this.

The value of $\bar{\nu}$ determined by this analysis for the entire fission spectrum is about 1.055 times $\bar{\nu}$ for thermal neutron fission in U^{235} . Leachman's calculations⁵ would indicate a $\bar{\nu}$ of 1.10 times the thermal $\bar{\nu}$ for U^{235} . This difference may or may not indicate a discrepancy between theory and experiment. We, of course, actually determine $\sigma^f (\bar{\nu}-1) - \sigma^c$ for the fission spectrum most exactly in our analysis and must know σ^f and σ^c to obtain $\bar{\nu}$. If the capture cross sections used are in error by 50 percent and if σ^f is in error by a few percent, then we could probably obtain a value for $\bar{\nu}$ which is 4.5 percent higher to agree with Leachman's calculations. The over-all uncertainty of $\bar{\nu}$ from this experiment and analysis is about 5 percent. Our $\bar{\nu}$ is, however, definitely in disagreement with that measured at Oak Ridge for monoenergetic neutrons.²¹ A numerical integration of these data gives a $\bar{\nu}$ for fission spectrum neutrons about 30 percent above the $\bar{\nu}$ for thermal neutrons.

The non-elastic cross section obtained for oralloy in group 3 is very nearly the same as that for tuballoy. Our σ_3^{ne} for oralloy is uncertain to 7 percent. In group 2, the oralloy non-elastic cross section is considerably higher than that for tuballoy, because of the large contribution of fissions, and it is uncertain to about 12 percent.

3.2 Non-elastic Cross Section and $\bar{\nu}$ for Oralloy at 4.0 and 4.5 Mev Neutron Energies

The $H^3(p,n)He^3$ neutron source was used to produce the 4.0 and 4.5 Mev neutrons for this sphere transmission investigation at the large Van de Graaff at Los Alamos. The

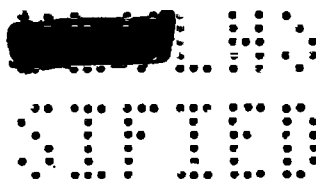
26


~~SECRET~~
S I T E D

experiment was routine, requiring no special corrections for background effects in the shell for the inelastic scattering determinations. The measurements were made with a 5 inch outside diameter, 3/8 inch thick shell of 94 percent enriched oralloy. As in Section 2.5 the cross section was determined for several energy thresholds of the detector. The non-elastic cross section is 3.34 ± 0.40 for both 4.0 and 4.5 Mev neutrons. Here the correction which must be made to the observed inelastic cross section, because fission neutrons from the shell are detected, is about 25 percent. Uncertainty in this correction is responsible for most of the experimental uncertainty. The evaluation of the measured transmissions was done by the Carlson S_4 method,⁹ assuming an external neutron source.

In order to determine values for $\bar{\nu}$ at 4.0 and 4.5 Mev neutron energy, sphere multiplications of a small oralloy sphere were performed with a "25" counter. Since the "25" counter is especially sensitive to low energy neutrons which might originate from room scattering, effects of this type were measured and removed experimentally from the observed multiplications. Statistical uncertainty in the multiplication measurements is responsible for 5 percent uncertainty in $\bar{\nu}$. Other uncertainties were such that the values of $\bar{\nu}$ given here have an overall uncertainty of about 10 percent. At 4.0 Mev the sphere multiplications give $\bar{\nu} = 3.13 \pm 0.31$ and at 4.5 Mev $\bar{\nu} = 3.26 \pm 0.33$. Ten percent is not the limiting precision which can be attained in this type of experiment. It appears, however, that 4 or 5 percent uncertainty is the limit if extreme care is taken. These values of $\bar{\nu}$ lie at present between those of the Diven-Terrell-Leachman group²² and those of J. L. Fowler²¹ of Oak Ridge.

0110
-37-
~~SECRET~~
S I T E D



Chapter 4

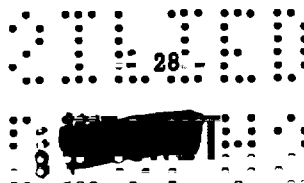
INELASTIC CROSS SECTIONS AND $\bar{\nu}$ FOR Pu²³⁹4.1 Fission Neutron Spectrum Results

The experiments and analysis of data for plutonium using a fission spectrum neutron source parallel those for or alloy in Chapter 3. The analysis uses Eqs. 3.1 through 3.4 to determine the same three unknowns as before, $\bar{\nu}$, σ_3^{in} and $\sigma_2^{\text{in}} + \sigma_2^{\text{c}}$. This analysis was also checked against S_4 calculations of sphere multiplications using the same input data. The transmissions calculated by the two different methods agreed to a few tenths of a percent. Auxiliary input data came from the same cross section sources as we used in Section 3.1.2.

The three quantities determined from our analysis for Pu²³⁹ are somewhat more uncertain than those obtained for or alloy. It will be recalled that the multiplication measured with a "25" detector determines $\bar{\nu}$, the average $\bar{\nu}$ for the fission neutron spectrum in plutonium. This quantity is about 5 percent uncertain. The sphere multiplication measured with the "28" detector gives the inelastic scattering plus capture cross section in energy group 3. This quantity is uncertain to about 15 percent. The sphere multiplication measured with the "37" detector gives the inelastic scattering plus capture cross section in group 2. This quantity is uncertain to about 25 percent.

Table 4.1 gives the three-group constants for Pu²³⁹ which best satisfy our multiplication measurements. These constants were used in an S_4 critical radius calculation. The radius which we obtain is 6.275 cm, whereas the measured radius of Jezebel (untamped critical mass of plutonium) was 6.285 cm. The effect due to the gallium (about 4 atomic percent) in the fabricated plutonium was put explicitly into the calculations (see Table 4.2). For the 200 MWD/T plutonium shells, we assumed that the Pu²⁴⁰ had the same cross sections as Pu²³⁹ since such a small amount of Pu²⁴⁰ was present. However, for the critical radius calculations, estimates²³ of the group fission cross sections of Pu²⁴⁰ were used, but the other constants for Pu²⁴⁰ were assumed to be the same as for Pu²³⁹.

The $\bar{\nu}$ for the fission spectrum is again (as for U²³⁵) only about 4 or 5 percent above the thermal $\bar{\nu}$ for plutonium. Leachman's predictions⁵ for plutonium indicate that $\bar{\nu}$ should be about 1.10 times the thermal $\bar{\nu}$. This difference is just inside of our experimental errors.



UNCLASSIFIED

TABLE 4.1

THREE-GROUP CROSS SECTIONS FOR Pu²³⁹*

Group 3 values		Group 2 values		Group 1 values	
σ_3^{tr}	4.66	σ_2^{tr}	5.53	σ_1^{tr}	8.39
σ_3^{f}	2.01	σ_2^{f}	1.80	σ_1^{f}	1.70
σ_3^{ne}	<u>2.85 ± 0.42</u>	σ_2^{ne}	<u>2.67 ± 0.66</u>	σ_1^{et}	6.40
σ_3^{et}	1.81	σ_2^{et}	2.87	σ_1^{c}	0.29
σ_3^{c}	0.04	σ_2^{c}	0.13	ν_1	2.90
σ_{32}^{in}	<u>0.45</u>	σ_{21}^{in}	<u>0.74</u>		
σ_{31}^{in}	<u>0.35</u>	ν_2	2.96	$\bar{\nu}$	<u>3.01</u>
ν_3	<u>3.05</u>				

*The underlined quantities are the ones primarily determined by the present measurements and computations.

TABLE 4.2

THREE-GROUP CROSS SECTIONS FOR GALLIUM

Group 3 values		Group 2 values		Group 1 values	
σ_3^{tr}	2.25	σ_2^{tr}	2.03	σ_1^{tr}	4.46
		σ_2^{ne}	0.27		
σ_3^{ne}	0.71	σ_2^{et}	1.76	σ_1^{et}	4.40
σ_3^{et}	1.54	σ_2^{c}	0.01	σ_1^{c}	0.06
σ_3^{c}	0	σ_{21}^{in}	0.26		
σ_{32}^{in}	0.47				
σ_{31}^{in}	0.24				

UNCLASSIFIED

~~SECRET~~
UNCLASSIFIED

4.2 Non-elastic Cross Sections and $\bar{\nu}$ at 4.0 and 4.5 Mev Neutron Energies

All sphere transmission runs were evaluated using the Carlson S_4 method⁹ to take into account multiple scattering and fission effects. Fission neutron detection was corrected for in our high energy threshold detector by the method given in Section 2.5. The non-elastic cross section for Pu^{239} is measured as 3.30 ± 0.35 barns at these two energies. The $\bar{\nu}$ determined from a "25" detector multiplication was 3.66 ± 0.40 . Leachman's calculations give 3.37 for $\bar{\nu}$. The non-elastic cross section for plutonium is influenced by the $\bar{\nu}$ which we use in the fission correction calculation. Since $\bar{\nu}$ is uncertain by 0.40, an uncertainty of 0.15 barns was introduced into the over-all uncertainty of the non-elastic cross section.

UNCLASSIFIED

~~SECRET~~

UNCLASSIFIED

Chapter 5

CONCLUSIONS

In the case of U^{238} , sufficient information is now available to allow one to determine the general shape of the variation of the inelastic collision cross section with energy (Fig. 2.2). The cross section behaves about like the other heavy elements tungsten and gold, rising quite rapidly to a fairly flat plateau region as more and more levels in the target nucleus become available for excitation by inelastic neutron scattering. The non-elastic cross sections for oralloy and Pu^{239} appear to be about the same as that for U^{238} at energies above approximately 2 Mev. In Table 5.1 the non-elastic cross sections for a fission spectrum and the U^{238} threshold detector are all within 9 percent of each other and the non-elastic cross sections at 4.0 or 4.5 Mev are within 6 percent of each other. However, in energy group 2 (0.4 to 1.4 Mev) one does not get the same values for the three isotopes, indicating at least some difference in the energy dependence of the inelastic cross section for the three isotopes at low energies.

We can conclude also that less than 20 percent of the inelastic scattering events in U^{238} occurring above the "28" detector threshold for a fission spectrum source produce neutrons that remain above the threshold, and this is probably true for oralloy and plutonium also. One can see this from the fact that the cross section for scattering below the "28" detector threshold for a fission spectrum is a large fraction of the inelastic cross section. For example, if one calculates the average non-elastic cross section of U^{238} measured with a "28" detector and fission spectrum neutron source by taking the appropriate average of the curve in Fig. 2.2, a cross section of 3.00 barns is obtained, while we measure 2.64 barns for the U^{238} non-elastic cross section in Section 2.1. The difference, 0.36 barns, represents the cross section, averaged over all neutrons initially above the "28" detector threshold, for such inelastic scatterings that leave them above the threshold.

It is possible to estimate the non-elastic cross sections for the fissionable isotopes considered in this report by extrapolating the curves of cross section vs $A^{2/3}$,^{1,2} to the appropriate values of $A^{2/3}$ for the various isotopes. The cross sections estimated by this method agree very well with the measured cross sections at all energies.

Three-group cross sections for U^{238} , oralloy and Pu^{239} have also been obtained, mainly from the shell multiplications with U^{238} , Np^{237} and U^{235} fission detectors. These three-group

UNCLASSIFIED

TABLE 5.1


PRIMARY QUANTITIES DETERMINED IN THE INVESTIGATION

Neutron energy	Isotope	σ_{ne}	$\sigma_3^{in} + \sigma_3^c$	$\sigma_2^{in} + \sigma_2^c$	σ_{31}^{in}	σ_{32}^{in}	$\bar{\nu}$	σ_3^{ne}	σ_2^{ne}
Fission spectrum	U ²³⁸		2.09 ± 0.11	0.86 ± 0.30	0.46 ± 0.35	1.59 ± 0.35		2.64 ± 0.13	0.86 ± 0.30
Fission spectrum	oralloy		1.35 ± 0.14	0.70 ± 0.25	0.42 ± 0.30	0.85 ± 0.30	2.60 ± 0.13*	2.59 ± 0.18	1.85 ± 0.22
Fission spectrum	Pu ²³⁹		0.84 ± 0.13	0.87 ± 0.25	0.35 ± 0.25	0.45 ± 0.25	3.01 ± 0.15*	2.85 ± 0.42	2.67 ± 0.66
4.0 and 4.5 Mev	U ²³⁸	3.16 ± 0.20					3.10 ± 0.40		
4.0 and 4.5 Mev	oralloy	3.34 ± 0.40					3.13 ± 0.31		
4.0 and 4.5 Mev	Pu ²³⁹	3.30 ± 0.35					3.26 ± 0.31		
							3.66 ± 0.40		

*Averaged over the fission spectrum.

UNCLASSIFIED

UNCLASSIFIED


SECRET

UNCLASSIFIED

cross sections have been tested to some extent by computing critical masses for oralloy and plutonium assemblies (Godiva and Jezebel).

A by-product of this investigation has been the determination of $\bar{\nu}$ for the fission spectrum and also 4.0 and 4.5 Mev monoenergetic neutrons in various fissionable isotopes. Unfortunately, the precision of these measurements has been only between 5 and 10 percent. Our values differ from those of Leachman⁵ and Diven and Terrell²² by about our experimental error. However, the experimental results given here are in definite disagreement with the $\bar{\nu}$ measurements for U²³⁵ reported in ORNL-1715.²¹ The problem of determining $\bar{\nu}$ from our multiplication measurements has also been taken up using the Monte Carlo method²⁴ of computing sphere multiplication. The results of this analysis are essentially in agreement with those given here.

The primary quantities determined in this investigation are collected in Table 5.1.

UNCLASSIFIED

SECRET



~~SECRET~~
SECRET

CLASSIFIED

REFERENCES

1. Bethe, Beyster, and Carter, LA-1429, January 1955.
2. Beyster, Henkel, Nobles, and Kister, Phys. Rev., 98, 1216 (1955).
3. E. T. Journey and C. W. Zabel, private communication.
4. R. B. Leachman and H. A. Schmitt, LA-1624, January 1953.
5. R. B. Leachman, internal Los Alamos document.
6. Brookhaven Cross Section Compilation, AECU-2040, November 1952.
7. Brookhaven Classified Cross Section Compilation, BNL-250, August 1954.
8. M. Walt and H. H. Barschall, TID-5157, 1953.
9. B. G. Carlson, LA-1599, October 1953.
10. M. Walt and J. R. Beyster, unpublished 1954 experiments.
11. P. Olum, Manhattan District Report MDDC-353 (LA-274), May 1945.
12. R. C. Allen and R. F. Taschek, unpublished except in M. Walt's report for 1955 International Conference on Peaceful Uses of Atomic Energy.
13. T. Bonner, unpublished.
14. E. R. Graves, Los Alamos Scientific Laboratory Report LAMS-1300, November 1951.
15. J. R. Beyster and M. Walt, unpublished 1955 experiments.
16. V. Weisskopf, private communication.
17. R. L. Henkel, LA-1493, November 1952.
18. H. H. Barschall and R. L. Henkel, LA-1714, August 1954.
19. G. E. Hansen and L. B. Engle, internal Los Alamos document; B. G. Carlson, internal Los Alamos document.
20. D. Okrent, R. Avery, and H. H. Hummell, report for 1955 International Conference on Peaceful Uses of Atomic Energy.
21. J. L. Fowler, Oak Ridge National Laboratory Report ORNL-1715, March 10, 1954.
22. H. C. Martin, J. Terrell, and B. C. Diven, internal Los Alamos document.
23. E. T. Journey, LA-1201, November 1950.
24. M. S. Goad, internal Los Alamos document.

CLASSIFIED

SECRET
~~SECRET~~

SECRET
CONFIDENTIAL

SECRET
CONFIDENTIAL